J. Nano- Electron. Phys.
3 (2011) No1, P. 302-307

PACS numbers: 81.05.Kf, 81.05.Gc 31.10.+ z, 82.80.Pv, 33.15.Fm

STRUCTURAL INVESTIGATION OF SBGESE GLASSES BY HIGH RESOLUTION X-RAY PHOTOELECTRON SPECTROSCOPY

***D.C. Sati*[1,2], *L.P. Purohit*[2], *R.M. Mehra*[3], *A. Kovalski*[1], *R. Golovchak*[1], *H. Jain*[1]**

[1] International Materials Institute for New Functionality in Glass,
Lehigh University, 18015, Bethlehem, PA, USA
E-mail: dineshsati05@yahoo.co.in

[2] Department of Physics,
Gurukula Kangri University, 249 404, Hardwar, India

[3] School of engineering and technology,
Sharda University, 201308, Greater Noida, India

The evolution of the structure of $Sb_8Ge_{32}Se_{60}$ *(*$Z = 2.72$*) and* $Sb_{20}Ge_{20}Se_{60}$ *(*$Z = 2.60$*) chalcogenide glasses is determined by high resolution X-ray photoelectron spectroscopy. Glasses with* $Z = 2.60$ *the structure consists of deformed tetrahedra and pyramids, in which at least one* Se *atom is substituted by* Ge *or* Sb *atom. For the* $Z = 2.72$ *structure consisting of shared pyramids and tetrahedra with two or more* Se *atoms substituted by the cations. At the same time,* Se-Se *dimers are present in both compositions.*

Keywords: *AMORPHOUS CHALCOGENIDE, X-RAY PHOTOELECTRON SPECTROSCOPY, CHEMICAL BONDS.*

(Received 04 February 2011, in final form 02 May 2011)

1. INTRODUCTION

The structure of chalcogenide glasses has been investigated extensively on the basis of random covalent network (RCN) model [1], chemically order network (CON) or chain crossing model [2], outrigger raft model [3] and topological model [4-6].

The RCN model treats the distribution of bonds as purely random, depending simply on the local coordination and the concentration of the constituent elements. Within the CON model for Se-rich compositions (i.e. $x < 1/3$), the Ge atoms are homogenously distributed throughout the Se matrix forming bonds with individual Se atoms and/or Se chains (-Se-Se-Se-) that are crosslinked via homogenously distributed $GeSe_4$ tetrahedra and are of the same constant length [7]. The formation of heteropolar Ge-Se bonds is preferred over the Se-Se homopolar bonds. The outrigger raft model is based on the existence of cluster of glass forming units. For the example of GeSe system, independent clusters of Se chains and edge shared GeSe4/2 tetrahedra form which would lead to phase separation. Philips [4] and Thorpe [5] have emphasized the role of the average coordination number (Z) in the determination of the structure, stability, optical and electronic properties of covalent glasses. The glass forming ability of a glass achieves maximum at $Z = 2.4$ which is called the rigidity percolation threshold.

Physically, at $Z = 2.40$, the network is supposed to be optimally coordinated to yield the best glass in the system for example $As_2Se(S)_3$, and $GeSe(S)_2$ is stochiometric composition. Tanaka [6] extended the Phillips and Thorpe idea by introducing another magic number. He investigate composition-dependence of the structural, elastic and electronics properties of chalcogenide glasses and suggested that ChG's undergo a structural phase transition at Z = 2.67. Using a network dimensionality approach, Tanaka explained that for Ge- and As-based ChG's the threshold at $Z = 2.67$ originates from a topological change from two-dimensional structures in materials of $Z \leq 2.67$ to three-dimensional structures for materials with $Z > 2.67$.

The physical and chemical properties of glasses are mainly determined by the atomic bonding and chemical composition. High-resolution X-ray photoelectron spectroscopy (HR-XPS) is very sensitive tool to determine the chemical environments and electronic states of elements in the compound. Change in structure by changing composition can have an influence on the optical and other properties.

In the present paper we examine a typical Sb-Ge-Se ternary chalcogenide glass system viz. $Sb_8Ge_{32}Se_{60}$ ($Z = 2.72$) and $Sb_{20}Ge_{20}Se_{60}$ ($Z = 2.60$), specifically the nonstoichiometric Ge_2Se_3 - Sb_2Se_3 cut across the glass-forming region.

2. EXPERIMENTAL

The samples of ternary $Ge_{40-x}Sb_xSe_{60}$ ($x = 8$, and 20) glasses were prepared by conventional melt-quench method from a mixture of high purity (99.9999) Ge, Sb and Se elements in evacuated quartz ampoules (at 10^{-6} Torr). The sealed ampoules were kept inside a rocking furnace at a temperature of 900 °C for 24 hour. The ampoules were quenched in ice cold water to form bulk glass.

High resolution XPS spectra were recorded with a Scienta ESCA-300 spectrometer using monochromatic AlK_α X-rays (1486.6 eV) under a vacuum of $2 \cdot 10^{-8}$ Torr or less. For all measurements the angle between the surface and detector was 90°. The XPS data consisted of survey scans over the entire binding energy range, and selected scans over the valence band or core level photoelectron peaks of interest. An energy increment of 1.0 eV was used for recording the survey spectra, 0.1 eV for valence band spectra and 0.05 eV for the case of core level spectra. The core level peak were recorded by sweeping the retarding field and using the constant pass energy of 150 eV, whereas for the valence band spectra we used 300 eV pass energy. The surface charging from photoelectron emission was neutralized using a low energy (< 10 eV) electron flood gun. The effective in minimizing distortions that might arise from differential surface charging on the surfaces, the use of flood gun results in the surface attaining a uniform though net negative potential with respect to the earth. The magnitude of this potential depends upon the geometry and conductivity of the surface. The $Ge_{30}Se_{70}$ film covered by gold (Au) was used as a reference [8].

Data analysis was conducted with standard CASA-XPS software package. For analyzing the core-level spectra, Shirley background was subtracted and a Voigt line shape was assumed for the peaks [9]. Each core-level spectrum for Sb, Ge and Se in our samples consisted of spin-orbit doublet components of d (i.e. $d_{5/2}$ and $d_{3/2}$) or p (i.e. $p_{3/2}$ and $p_{1/2}$) levels. The number of

doublets within a given peak was determined by an iterative curve fitting procedure in which a doublet was added only if it significantly improved the goodness of the fit. The full width at half maximum (FWHM) was assumed to be the same for the peaks within one doublet. However different FWHM values were allowed for independent doublets of the same core-level peak. The mix between the Gaussian and Lorentzian in the Voigt function was chosen to be the same for all doublets of a given core-level. The fitting procedure gave mix values close to 90 % Gaussian and 10 % Lorentzian and asymmetry values close to zero for all peaks. The uncertainties in the peak position and area of each component were ± 0.05 eV and ± 2 % respectively.

3. RESULT AND DISCUSSION

A typical XPS survey spectrum of the $Sb_{20}Ge_{20}Se_{60}$ bulk glasses is shown in Fig. 1.

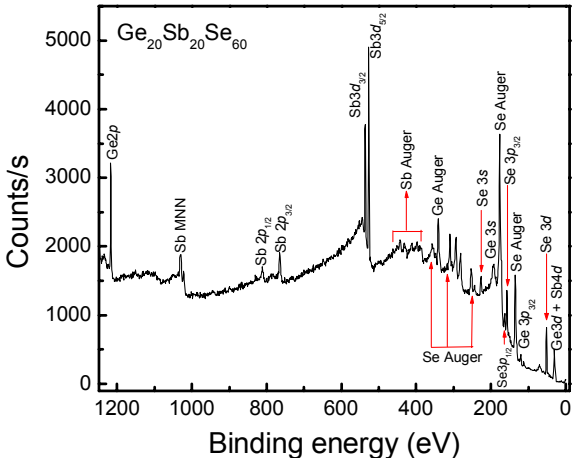

Fig. 1 *– Survey XPS spectrum of* $Sb_{20}Ge_{20}Se_{60}$ *bulk glass*

The well defined peaks are visible for Sb, Ge and Se core levels and also related Auger lines. No elements other than the glass components are observed in such spectra.

More precise information about the structure of $Sb_8Ge_{32}Se_{60}$ ($Z = 2.72$) and $Sb_{20}Ge_{20}Se_{60}$ ($Z = 2.60$) can be obtained by analyzing the core-level XPS spectra. The fit parameters, such as BE, FWHM and partial area (A) for various components are given in Table 1. Since both investigated materials are Se-poor compositions and belong to Sb_2Se_3-Ge_2Se_3 (so-called non-stoichiometric) cut-line of the glass-forming region, only Ge-Se-Ge, Ge-Se-Sb and Sb-Se-Sb fragments are expected for nearest neighbor environment around Se atoms. Owing to close electronegativity values of Sb and Ge (2.05 and 2.01, respectively [10]), these environments should result in very similar chemical shifts and, consequently, can not be unambiguously resolved in the Se 3d core-level spectrum, thus resulting as one component in the spectrum. Experimental spectra of Se 3d core level and their best fit component peaks are shown in Fig. 2 for the present compositions. Contrary to the expectations, the Se 3d core level spectra of the investigated samples can not be fitted using just one doublet (see Fig. 2 and Table 1).

Two doublets with primary (i.e. $3d_{5/2}$) component at 54.10 (± 0.05) and 53.70 (± 0.05) eV need to be introduced into the envelope of fitting curve to obtain acceptable quality of the fit. Owing to their positions and moieties, the doublet with primary component at ~ 53.70 eV is attributed to the mixed (Sb/Ge)-Se-(Sb/Ge) and the one at 54.10 eV to Se-Se-(Sb/Ge) environments. The latter fragment includes Se-Se dimers that are not to be expected in these Se deficient compositions. Higher FWHM values (~ 0.8-0.9 eV) for these doublets in comparison to those of binary Ge-Se chalcogenide glasses (~0.6-0.7 eV) [11] just confirm that the contribution from mixed Ge and Sb neighbors are similar but not exactly the same. To understand the above features of the investigated samples, complementary information can be obtained from the analysis of Sb and Ge core levels. Experimental spectra of Se 3*d* core level and their best fit component peaks are shown in Fig. 2.

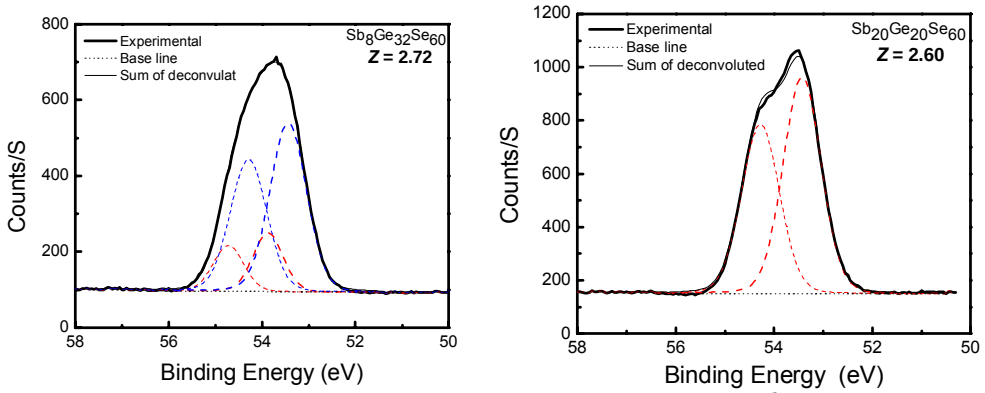

Fig. 2 *– Deconvolution of Se 3d core level spectra for* $Sb_8Ge_{32}Se_{60}$ *(a) and* $Sb_{20}Ge_{20}Se_{60}$ *glasses (b) (dashed lines correspond to best fit doublet components)*

Table 1 *– Best fit values of characteristic parameters of Se 3d (*$3d_{5/2}$ *component) core level peaks (the analyzed core level is written in bold font)*

Composition /core level	*Z*	Se-Se-Ge(Sb)			(Sb)Ge-Se-Ge(Sb)		
		BE	fwhm	*A*	BE	fwhm	*A*
$Sb_8Ge_{32}Se_{60}$	2.72	54.12	0.80	32	53.69	0.89	68
$Sb_{20}Ge_{20}Se_{60}$	2.60	53.94	0.72	32	53.61	0.86	68

Fig. 3 shows partially overlapped Sb 4*d* and Ge 3*d* core level spectra for the investigated compositions and their best fit components. Fitting parameters are given in Table 3. According to these results (Table 2), the Ge 3*d* core level spectrum can be fitted by just one doublet with primary component at 30.30 (± 0.05) eV in the case of $Sb_{20}Ge_{20}Se_{60}$ with $Z = 2.60$. Because our glasses belong to the non-stoichiometric Sb_2Se_3-Ge_2Se_3 cut-line of the glass-forming region, homopolar Ge-Ge bonds are unavoidable in their structure. So, the observed doublet at 30.30 eV with a high probability should be attributed to the deformed tetrahedra, where one of the chalcogen atoms is substituted by Ge atom. Instead of Ge atoms, the substitution can be realized also by Sb atoms of very similar electronegativity value. On the other hand, Ge 3*d* core level peak for $Sb_8Ge_{32}Se_{60}$ glass with $Z = 2.72$

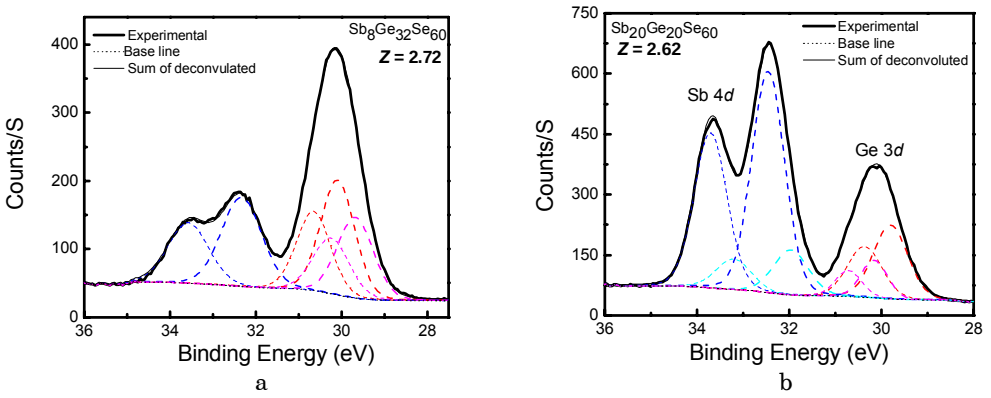

Fig. 3 – *Deconvolution of Ge 3d and Sb 4d core level spectra for* $Sb_8Ge_{32}Se_{60}$ *(a) and* $Sb_{20}Ge_{20}Se_{60}$ *glasses (b) (dashed lines correspond to best fit doublet components)*

consists of two doublets. There is an additional doublet with primary component at 29.90 (± 0.05) eV in the envelope of the fitted curve, which arises with the further substitution of Se atoms in Ge-based tetrahedra by Sb or Ge cations.

For the $Sb_{20}Ge_{20}Se_{60}$ glass the Sb 4*d* core level spectrum could be fitted by one doublet, with primary component at 32.70 (± 0.05) eV (Table 2). Significant concentration of Se-Se dimers as established from the analysis of Se 3*d* core level spectrum of this glass can be achieved only if the presence of cation (Sb or Ge) is assumed as the nearest neighbor of Sb atoms.

The existence of Sb-Sb bonds in the structure of $Sb_{20}Ge_{20}Se_{60}$ glass can be inferred from the neutron diffraction studies [12]. So, the observed doublet may be attributed to deformed Sb-based pyramids, where one of Se atoms is substituted by Sb or Ge cations. To obtain a reasonable fit of Sb 4*d* core level XPS spectra of $Sb_8Ge_{32}Se_{60}$ samples, additional doublet with primary component at ~ 32.20 (± 0.05) eV (Table 2) must be introduced into the envelop of fitted curve. Owing to its BE this component of Sb 4*d* core level spectrum for compositions around $Z = 2.72$ can be attributed to further deformation of Sb-based pyramids by substitution of two and more Se atoms with Ge or Sb cations. Simultaneous presence of Se-Se dimers as determined from the analysis of Se 3*d* core level spectrum of these glasses just confirms the conclusion.

Table 2 – *Best fit values of characteristic parameters of Ge* $3d_{5/2}$ *and Sb* $4d_{5/2}$ *components of core level spectra (the analyzed core level is written in bold font)*

Composition /core level	Z	(Ge,Sb)-Ge-$(Se)_3$			$(Ge,Sb)_2$-Ge-$(Se)_2$		
		BE	fwhm	A	BE	fwhm	A
$Sb_8Ge_{32}Se_{60}$	2.72	30.31	0.99	78	29.85	0.99	22
$Sb_{20}Ge_{20}Se_{60}$	2.60	30.22	0.93	100			

Composition /core level	Z	Se-Sb-$(Se)_2$			Sb-Sb-$(Se)_2$		
		BE	fwhm	A	BE	fwhm	A
$Sb_8Ge_{32}Se_{60}$	2.72	32.76	0.99	75	32.28	0.92	25
$Sb_{20}Ge_{20}Se_{60}$	2.60	32.71	0.93	100			

So, we do not have either regular $SbSe_{3/2}$ pyramids or regular $GeSe_{4/2}$ tetrahedra in a high concentration in both glasses. According to present HR XPS data the increase in glass connectivity through $Z = 2.67$ point leads to a gradual replacement of one or more Se atoms in pyramids or tetrahedra with Ge or Sb cations. At the same time the concentration of Se-Se dimers remains practically unchanged at the level of ~30 % of Se atoms (Table 1). Therefore, the formation of ethane-like $Ge_2(Se_{1/2})_6$ units, proposed recently to explain the glass-formation in Ge-rich chalcogenide glasses [13], is a plausible picture for $Sb_{20}Ge_{20}Se_{60}$ glass with $Z = 2.60$.

4. CONCLUSION

From the analysis of Sb, Ge and Se core level XPS spectra, we conclude that the structure of Se-poor glasses within the nanoscale phase separated region of $Sb_xGe_{40-x}Se_{60}$ family exhibits distinct patterns. Formation of the deformed Ge-based tetrahedra and Sb-based pyramids where one of the chalcogen atoms is substituted by Ge or Sb cation, prevails for the glasses with $Z = 2.60$. Approaching the transition point at $Z = 2.72$ domain, more than one Se atoms in pyramids or tetrahedra are replaced with Ge or Sb cations.

REFERENCES

1. W.H. Zacharmsen, *J. Am. Chem. Soc.* **54**, 3841 (1932).
2. G. Lucovsky, F.L. Galeener, R.C. Keezer, R. H. Geils, H.A. Six, *Phys. Rev. B* **10**, 5134 (1974).
3. P.M. Bridenbaugh, G.P. Espinosa, J.E. Griffiths, J.C. Phillips, J.P. Remeika, *Phys. Rev. B* **20**, 4140 (1979).
4. J.C. Phillips, *J. Non-Cryst. Solids* **34**, 153 (1979).
5. M.F. Thorpe, *J. Non-Cryst. Solids* **57**, 355 (1983).
6. K. Tanaka, *Phys. Rev. B* **39**, **1270** (1989).
7. B. Bureau, J. Troles, M.Le Floch, F. Smektala, J. Lucas, *J. Non-Cryst. Solids* **326- 327**, 58 (2003).
8. A. Kovalskiy, A.C. Miller, H. Jain, M. Mitkova, *J. Am. Ceram. Soc.* **91**, 760 (2008).
9. J.D. Conny, C.J. Powell, *Surf. Interface Anal.* **29**, 856 (2000).
10. L. Pauling, *The Nature of the Chemical Bond*, (Cornell Univ. Press: Ithaca: 1960).
11. R. Golovchak, O. Shpotyuk, S. Koziukhin, A. Kovalskiy, A.C. Miller, H. Jain, *J. Appl. Phys.* **105**, 103704 (2009).
12. S. Neov, I. Gerasimova, E. Skordeva, D. Arsova, V. Pamukchieva, P. Mikula, P. Lukas, R. Sonntag, *J. Mater. Sci.* **34**, 3669 (1999).
13. Y. Skaguchi, D.A. Tenne, M. Mitkova, *J. Non-Cryst. Solids* **355**, 1792 (2009).